Nanoscale



PAPER

View Article Online

View Journal | View Issue



Cite this: *Nanoscale*, 2020, **12**, 23036

Synthesis of vulcanite (CuTe) and metastable Cu_{1.5}Te nanocrystals using a dialkyl ditelluride precursor†

Evan H. Robinson, Da,b Kaelyn M. Dwyer, Da Alexandra C. Koziel, Da,b Ahmed Y. Nuriye Cand Janet. E. Macdonald Da,b

This study demonstrates that a dialkyl ditelluride reagent can produce metastable and difficult-to-achieve metal telluride phases in nanocrystal syntheses. Using didodecyl ditelluride and without the need for phosphine precursors, nanocubes of the pseudo-cubic phase (Cu_{1.5}Te) were synthesized at the moderate temperature of 135 °C. At the higher temperature of 155 °C, 2-D nanosheets of vulcanite (CuTe) resulted, a nanomaterial in a phase that has not been previously achieved through thermal decomposition methods. Materials were characterized with TEM, powder XRD and UV-Vis-NIR absorbance spectroscopy.

Received 26th September 2020, Accepted 2nd November 2020 DOI: 10.1039/d0nr06910h

rsc.li/nanoscale

1. Introduction

Copper(I) telluride nanocrystals (NCs) are an emerging member of the copper chalcogenide nanomaterial family and, like the corresponding sulfides and selenides, ^{1,2} copper telluride has an advantageous capacity for facile cation exchange. ^{3,4} Additionally, copper telluride is a direct bandgap semiconductor (1.1–1.5 eV) and the copper vacancies in substoichiometric Cu_{2-x}Te phases give those materials plasmonic properties. ⁵⁻⁷ While not as prevalent in the literature as their sulfide or selenide counterparts, the copper tellurides have generated interest for their optical, ^{3,8,9} photothermal, ^{5,10,11} thermoelectric, ^{12,13} photocatalytic, ¹⁴ and electrochemical properties. ¹⁵ The Cu–Te phase diagram is noted for being extremely complex with seven known compounds, most of which are polymorphic. ^{16,17} Although numerous, little is known about the properties of many of these phases.

Early literature examples of copper telluride nanoscale materials dating to the first decade of the 2000s featured microwave-based syntheses syntheses and hydrothermal methods. These syntheses used elemental Te as a reagent and primarily resulted in crystalline aggregates of the hexag-

onal mineral phase weissite, Cu₂Te. Several copper deficient Cu_{2-x} Te phases are known in the bulk phase diagram. However, in 2013, Li, et al. published a synthesis for colloidal copper telluride nanocrystals in a pseudo-cubic phase that did not match any existing known structures using lithium bis(trimethylsilyl) amide as a precursor activating agent and trioctylphosphine telluride (TOP:Te) as a tellurium source.⁵ The authors were able to synthesize cubes, platelets and nanorods of this (at that time) unidentified metastable copper telluride phase. This pseudo-cubic phase—later called "Cu_{1.5}Te" by Mugnaioli, et al., 22 and forthwith in this article—has been since synthesized and reported in other instances in the literature using the same tellurium source, 5,10 but not definitively characterized until aberration-corrected TEM analysis was performed by both Willhammar, et al.,8 and later Mugnaioli, et al. 22 The orthorhombic unit cell (a = 7.5(1) Å, b = 22.8(2) Å, c= 29.6(3) Å) consists of 96 Te atoms arranged in a pseudo-cubic lattice with 124 Cu atoms tetrahedrally coordinated by Te, giving a formula of Cu_{1.3}Te. The designation of this phase "Cu_{1.5}Te" is somewhat nominal and a range of stoichiometries have been observed.^{5,22}

Also difficult to synthesize as nanomaterials is the copperdeficient phase vulcanite (CuTe), which has a layered structure. It can be approximately described as having hcp stacked Te with copper filling all of the tetrahedral holes, but only in alternating close packed layers.²³ Vulcanite has a modest presence in the literature, and the bandgap of 1.5 eV suggests possible application in photovoltaics, and the mineral is also highly birefringent and pleochroic. Much of the research on this phase is devoted to studying the properties of CuTe thin films.²⁴ As a layered structure, it has potential as a new 2D

^aDepartment of Chemistry, Vanderbilt University, Nashville, Tennessee 37235, USA. E-mail: janet.macdonald@vanderbilt.edu

^bThe Vanderbilt Institute of Nanoscale Science and Engineering, Vanderbilt University, Nashville, Tennessee 37235, USA

^cDepartment of Chemistry, The Pennsylvania State University, Abington College, 1600 Woodland Road, Abington, Pennsylvania, 19001, USA. E-mail: auy3@psu.edu †Electronic supplementary information (ESI) available. See DOI: 10.1039/d0nr06910h

Nanoscale Paper

material. While vacuum and electrochemical depositions of CuTe are known, ^{25–27} a traditional nanocrystal synthesis is absent from the literature.

We and others, especially the Brutchey group, 28,29 have found success in using alkyl selenide reagents to achieve phase control in the synthesis of binary and ternary copper chalcogenide NCs, specifically targeting metastable (higherenergy 30) crystal phases. In a previous publication from our group, an n-alkyl diselenide precursor was used to directly synthesize a unique phase of hexagonal-like Cu_{2-x}Se that is not known in the bulk, 31 and had only been reported once previously through cation exchange. 32 In contrast, using n-alkyl selenol yielded the thermodynamic cubic Cu_{2-x}Se phase. This article discusses the application of a similar ditelluride precursor in the synthesis of metastable $\text{Cu}_{1.5}\text{Te}$ nanocrystals and difficult-to-achieve CuTe nanosheets, thereby avoiding the use of phosphines or electrochemical techniques.

2. Experimental

2.1 Materials

Dioctyl ether (DOE, 99%), oleic acid (OA, 90%, technical grade), 1-octadecene (ODE, 90% technical grade), oleyl amine (OlAm, 70%, technical grade) were obtained from Sigma-Aldrich. Copper(II) acetylacetonate (Cu(acac)₂, >98%) was obtained from Strem Chemicals. Tellurium powder (200 mesh, 99.5% metals basis), 1-bromododecane (98%), dimethylformamide (99.8%) were obtained from Fisher Scientific. Hexanes (ACS grade, 98.5%) was obtained from VWR. All materials were used as received without additional purification.

2.2 Synthesis of didodecyl ditelluride

This synthesis was adapted from the work of Li, et al.³³ A mixture of Te powder (3 g, 23.6 mmol) and NaBH₄ (0.71 g) in 30 mL dimethylformamide (DMF) was refluxed at 85 °C for 20 minutes. Separately, 5.67 mL (23.6 mmol) of 1-bromododecane was mixed with 10 mL of DMF, added to the dark purple solution and stirred for 3 hours. The mixture was filtered to remove unreacted Te, and the red solution was extracted with hexane/water. Hexane was evaporated to leave a solid brick-red product of didodecyl ditelluride (DD₂Te₂). The product can decompose to a grey material over the process of months when stored in a vial on a lab bench. To slow decomposition, the material is stored wrapped in aluminum foil to limit light exposure.

2.3 Synthesis of copper telluride nanocrystals

Standard Schlenk line techniques were used throughout with Ar as the inert gas. In a typical heat-up synthesis, 0.55 mmol of didodecyl ditelluride, 0.25 mmol of Cu(acac)₂, and 2.5 mL of solvent (ODE, OlAm, OA, DOE) were mixed in a 25 mL 3-necked flask. The flask was put under vacuum and the temperature was raised to 80 °C for 30 min. Then the flask was put under inert atmosphere and the temperature was raised to the

reaction temperature of 135 or 155 °C. The reaction flask was held at temperature from 30 to 60 minutes. The flask was allowed to cool to room temperature, and the post-reaction mixture was precipitated in acetone three times and resuspended in chloroform.

2.4 Synthesis of CuTe nanosheets

Standard Schlenk line techniques were used throughout with Ar as the inert gas. In a typical heat-up synthesis, 0.25 mmol of didodecyl ditelluride, 0.25 mmol of Cu(acac)₂, and 2.5 mL of dioctyl ether were mixed in a 25 mL 3-necked flask. The flask was put under vacuum and the temperature was raised to 80 °C for 30 min. Then the flask was put under inert atmosphere and the temperature was raised to the reaction temperature of 155 °C. The reaction flask was held at temperature for 60 minutes. The flask was allowed to cool to room temperature, and the post-reaction mixture was precipitated in acetone three times and resuspended in chloroform.

2.5 Synthesis of CuTe nanosheets from Te(0) intermediate

Standard Schlenk line techniques were used throughout with Ar as the inert gas. In a typical heat-up synthesis, 0.55 mmol of didodecyl ditelluride and 2.5 mL of dioctyl ether were mixed in a 25 mL 3-necked flask. The flask was put under vacuum and the temperature was raised to 80 °C for 30 minutes. Then the flask was put under inert atmosphere and the temperature was raised to the reaction temperature of 155 °C for 1 hour. The solution turned dark orange and then 0.25 mmol of Cu(acac)₂ was dissolved in a minimum of DOE and injected into the reaction flask. The reaction was held at 155 °C for 1 hour. The flask was allowed to cool to room temperature, and the post-reaction mixture was precipitated in acetone three times and resuspended in chloroform.

2.6 Characterization

Transmission Electron Microscopy (TEM) was performed on a FEI Technai Osiris digital 200 kV S/TEM system. Absorption spectra were obtained on a Jasco V-670 UV-Vis spectrophotometer. X-ray diffraction (XRD) measurements were performed using a Rigaku SmartLab powder X-ray diffractometer with a CuK α ($\lambda=0.154$ nm) radiation source set to 40 kV and 44 mA, and a D/teX Ultra 250 1D silicon strip detector. XRD patterns were acquired using a step size of 0.1 degrees at 1 or 10 degrees per minute.

2.7 Computational methods

The computational methods performed herein were adapted from the works of Guo *et al.*³⁴ and Rhodes *et al.*³⁵ Bond dissociation energies were calculated using Gaussian 16 with density functional theory (DFT) and the Boese–Martin kinetics (BMK) functional. Molecular geometry optimization was performed using the def2SVPD basis set which includes a 28-electron pseudopotential on tellurium, and single-point energy calculations were performed using the def2TZVPD basis set with the same pseudopotential on tellurium.

Paper Nanoscale

3. Results and discussion

Copper telluride NC syntheses were adapted from the analogous selenide-based procedure of Hernandez-Pagan, et al. 31 In a typical synthesis, 0.25 mmol of Cu(acac)2, 0.55 mmol DD2Te2 and 5 mL of either oleylamine (OlAm), oleic acid (OA), octadecene (ODE) or dioctyl ether (DOE) were mixed in a threenecked flask. Following standard Schlenk line techniques, precursors were degassed at 80 °C for 30 minutes then heated to the reaction temperature of 135 °C or 155 °C for 30 min-1 h. The crystalline products were precipitated in polar solvents and resuspended in chloroform.

As shown in Fig. 1, nanocrystals synthesized at 135 °C for 30 minutes varied in size depending on the solvent present in addition to DD2Te2; reactions with coordinating species of OlAm or OA resulted in nanocrystals of cuboid morphology. Nanocrystals synthesized in OlAm (Fig. 1A) had edge lengths measuring 10.2 ± 1.4 nm (N = 150). In addition, these colloidal NCs exhibited a plasmonic absorption feature in the near-IR centered at approximately 950 nm (Fig. 1D), similar to those described by Li, et al.5 NCs synthesized in OA shared the cubelike morphology, though were considerably larger with edgelengths of 36 \pm 7 nm (N = 150). When ODE was used, the product crystals were rectangular prismatic with the longest dimensions approaching the micron scale. The particles, due to their large size, were not colloidally stable (Fig. 1C). Powder X-ray diffractometry (XRD) revealed the metastable pseudocubic phase Cu_{1.5}Te was the product in all three cases (Fig. 1E). EDS revealed that in oleylamine and oleic acid, the stoichiometry was very close to Cu_{1.5}Te, and in ODE the stoichiometry more closely matched the calculated structural formula at Cu_{1.15}Te. As previously mentioned, multiple stoichiometries for this phase have been observed before and the factors leading to this variability and their structural and functional consequences are not understood.

When DOE was used as the solvent in the synthesis, the NCs were qualitatively similar to the ODE-synthesized product in Fig. 1C. However, nanoribbons were sporadically distributed among the NCs when characterized with TEM. Fig. 2A highlights a solitary nanoribbon that measured approximately 3 µm in length and approximately 50 nm at the wider of the two ends. As depicted in Fig. 2B, extending the reaction time to 1 hour increased the prevalence and size of the nanosheets (Fig. 2B nanosheet measured to approximately 4.2 µm long and 350 nm wide). Upon increasing the reaction temperature to 155 °C (for 1 hour), the smaller cube-like NCs seen at lower temperatures were no longer observed by TEM. Instead, the nanosheet morphology dominated in the TEM micrographs (Fig. 2C).

XRD characterization of the samples synthesized in DOE revealed the presence of the pseudo-cubic phase of Cu_{1.5}Te (Fig. 2D, 30 min at 135 °C). However, with increasing time and temperature the vulcanite (CuTe) phase becomes the dominant copper telluride crystal structure, with a Te(0) impurity

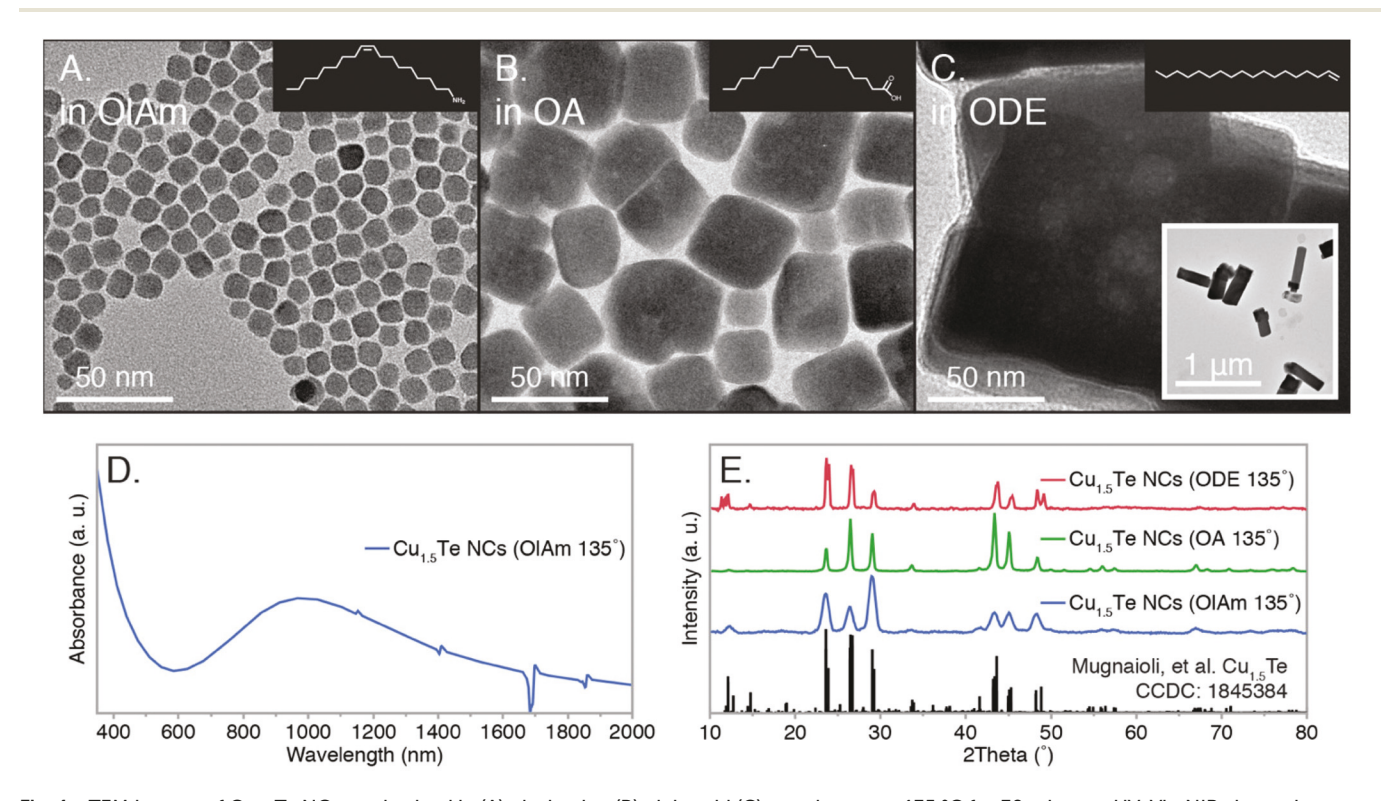


Fig. 1 TEM images of Cu_{1.5}Te NCs synthesized in (A) oleylamine (B) oleic acid (C) octadecene at 135 °C for 30 minutes. UV-Vis-NIR absorption spectrum (D) of colloidal NCs synthesized in OlAm reveals a plasmonic absorption feature at centred at approximately 950 nm. Powder XRD patterns (E) were indexed to the pseudo-cubic crystal structure of Cu_{1.5}Te described by Mugnaioli, et al. (CCDC: 1845384†).

Nanoscale

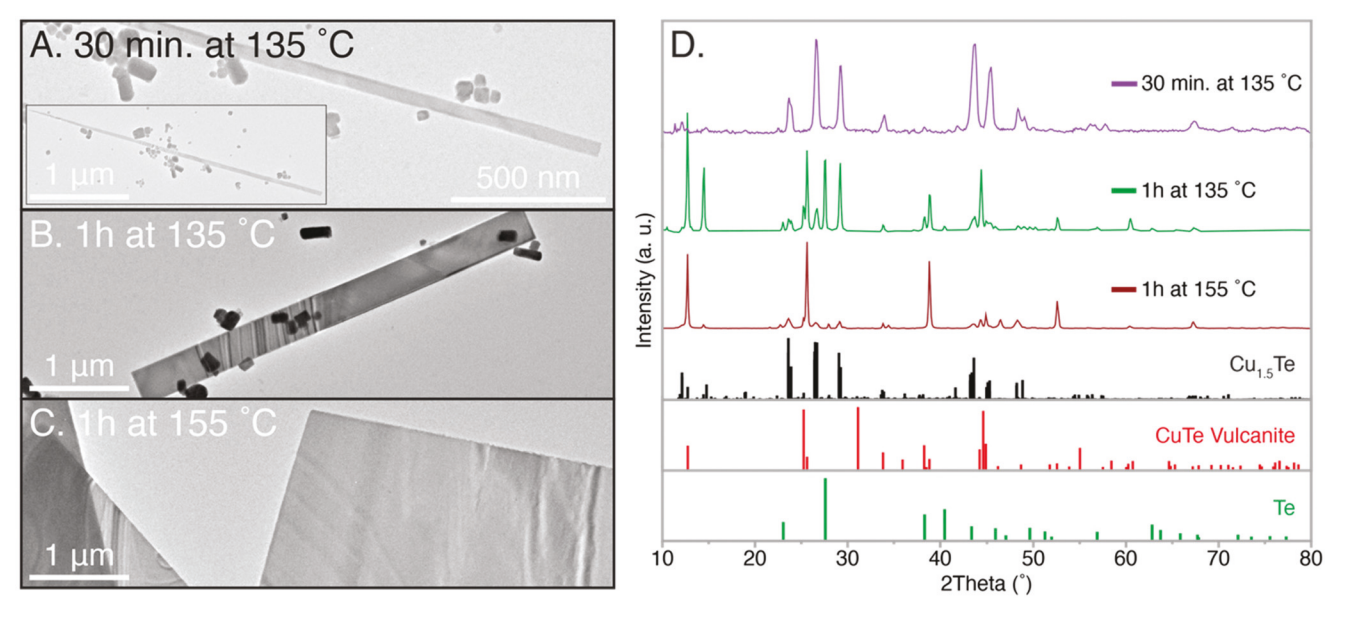


Fig. 2 TEM images of copper telluride NCs synthesized in DOE at (A) 135 °C for 30 minutes (B) 135 °C for 1 hour (C) 155 °C for 1 hour at the same scale for comparison. XRD patterns (D) of the samples synthesized under different reaction conditions. Note that the XRD pattern for 1 h at 155 °C represents a product formed with 1:1 Cu(acac)₂: DD₂Te₂ and can be identified as primarily vulcanite with a small Cu_{1.5}Te impurity. Cu_{1.5}Te reference pattern from Mugnaioli, et al. (CCDC: 1845384†), vulcanite (CuTe, ICSD: 93966), and Te(0) (ICSD: 65692).

(Fig. S1†). As shown in Fig. 2D for the sample obtained at 1 h at 155 °C, decreasing the Te: Cu ratio from 2:1 to 1:1 prevented the formation of the Te(0) impurity. Sharp, but weak reflections at 25° (011) and 31° (101), a missing reflection at 37° (110) and unexpectedly strong reflections at 26° (002) and 39° (003) for the vulcanite product suggests a strong preferred orientation effect with the c-direction normal to the sample stage. This is consistent with the sheet morphology seen by TEM (Fig. S2†).36

As shown in Fig. 3, high-resolution TEM and subsequent FFT analysis also supported the identification of the nanosheets as vulcanite, with the growth directions running parallel to the layered structure of that particular phase. Specifically, growth occurred along the <200> and <020> directions, which run orthogonal to the stacked CuTe crystal structure. Quantitative EDS characterization of regions of the nanosheet product revealed a copper rich stoichiometry with

58-74% Cu, suggesting the presence of unreacted copper precursor or possibly a copper-rich surface chemistry.

As stated above, the work presented here follows our previous publication on phase control of Cu2-xSe NCs with DD₂Se₂ and DDSeH. Following that work, an analogous comparison with DDTeH was pursued, but the tellurol proved susceptible to oxidation, ^{28,37} preventing facile handling.

Both the DD₂Se₂ and the DD₂Te₂ produced NCs with metastable phases not known in the bulk of Cu_{2-x}Se and Cu_{1.5}Te, respectively. One hypothesis is that these alkyl dichalcogenide reagents or their decomposition products also provide a specialized surface ligation that aids stabilization of one phase over another. Observations in CdSe have shown that X-type ligation favours cubic zinc blende because of its four positively charged [111] facets, whereas hexagonal wurtzite only has the one (002). L-Type ligation therefore favours wurtzite. 38-41 Interestingly, here the metastable phase for the copper sele-

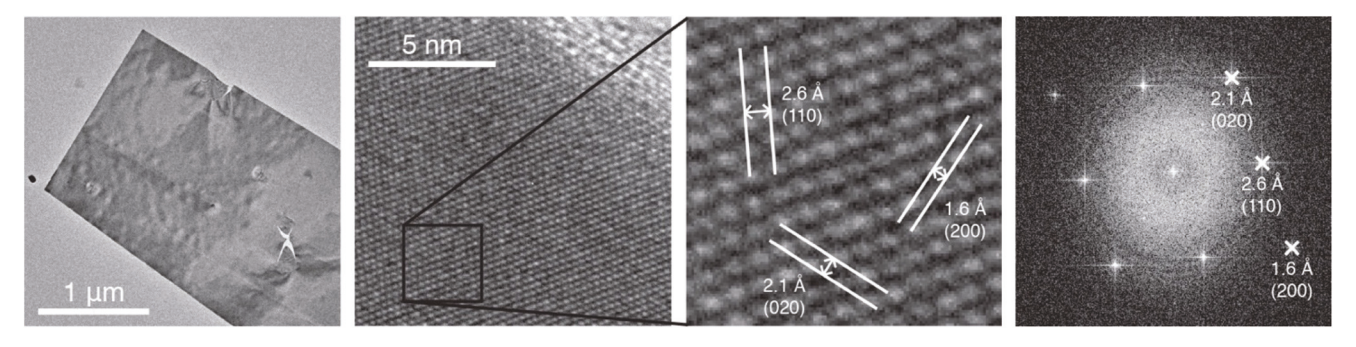


Fig. 3 TEM images of a copper telluride nanosheet with HR-TEM image (and Right: corresponding FFT analysis) indexed to vulcanite CuTe (ICSD: 93966).

Paper

nide is pseudo-hexagonal and the bulk phase is cubic, whereas it is reversed for the telluride; the metastable $Cu_{1.5}$ Te phase is pseudo-cubic, and the bulk Cu_2 Te and Cu_{2-x} Te phases are hexagonal. This suggests that the role of the dichalcogenide precursors is not a special surface ligation that might be consistent across dialkyl dichalcogenides.

Another hypothesis as to why dialkyl dichalcogenide reagents are giving nanomaterials in metastable phases is that the effect is kinetic, following Ostwald's rule of stages where metastable materials always form first before transforming into the thermodynamic phase. As has been seen with CdSe NCs, slow reaction kinetics allow the particles formed to be relatively free of the defects and stacking faults that can catalyse transformations to the thermodynamic phase. Controlled reaction kinetics can therefore trap metastable phases in nanocrystal synthesis. 42,43

Further comparison reveals that the higher reactivity of the ditelluride over the selenide facilitated lower synthesis reaction temperatures (135 °C ν s. 155 °C). The calculated C–Te BDE value for a dialkyl ditelluride (37.4 kcal mol⁻¹, Fig. S3†) shows the C–Te bond is substantially weaker than the previously published dialkyl diselenide analogue (C–Se: 55.4 kcal mol⁻¹). The weaker C–Te bond of DD₂Te₂ results in markedly different crystallite sizes in comparison to the diselenide/Cu_{2–x}Se NCs. The previously reported WZ Cu_{2–x}Se NCs synthesized in ODE at 155 °C for 1 hour were disk-shaped with diameters of approximately 14 nm. Cu_{2–x}Te NCs synthesized here in ODE at a lower temperature for less time were approaching a micron in length (Fig. 1C).

The highly reactive ditelluride precursor enabled the growth of nanosheets of CuTe at elevated reaction temperatures; an analogous material was not observed in the $\mathrm{Cu}_{2-x}\mathrm{Se}$ investigation. Nanosheets of hexagonal $\mathrm{Cu}_2\mathrm{Te}$ and the pseudocubic phase $\mathrm{Cu}_{1.5}\mathrm{Te}$ have been synthesized previously, however the preparation of 2-dimensional vulcanite CuTe nanoribbons has required electrochemical growth on electrodes. As

The Te(0) impurity seen with the CuTe nanosheets in Fig. S1† suggests that at 155 °C, the DD₂Te₂ can decompose to release Te(0) and may be active in the phase selection of CuTe. In a control reaction, the ditelluride precursor was heated alone to nucleate Te(0) NCs followed by the injection and reaction of the copper precursor. No copper telluride resulted and only Te(0) was identified by XRD and TEM (Fig. S4†). It can be concluded that intermediate Te(0) nanocrystals formed in situ are unlikely to be the active reagent in the phase determination of CuTe. Furthermore, previous preparations of copper telluride using either Cu(I) or Cu(0) reagents with Te(0) produced Cu2Te rather than CuTe. The mechanism to produce CuTe presented here likely involves the reaction of Cu¹⁺ directly with DD₂Te₂ through a new decomposition route that is only accessible at the high reaction temperature of 155 °C and not 135 °C. The DD₂Te₂ precursor is mimicking electrochemical reduction syntheses of vulcanite CuTe nanomaterials in a way that is not achieved when elemental Te or TOP: Te is used as an NC precursor, as those produced Cu2Te and

 ${
m Cu}_{1.5}{
m Te}$, respectively. $^{5,18-22}$ We can postulate that the ditelluride is unique among these reagents in its ability to template Te–Te bonding between layers seen in the vulcanite structure. It should be noted that even the electrochemical routes to CuTe often require repeated atomic layer depositions or very high pH. 26,44 The Pourbaix diagram 45 for Te suggests the high pH stabilizes ${
m Te}_2{
m ^{2-}}$ units in those cases to template the interlayer bonding of vulcanite. The ${
m DD}_2{
m Te}_2$ has truly unique characteristics as a reagent to access metastable phases.

4. Conclusions

In summation, Cu_{2-x} Te NCs were synthesized using didodecyl ditelluride as the tellurium precursor. In the solvents OlAm, OA, ODE and DOE, the pseudo-cubic phase $Cu_{1.5}$ Te and a cube-like morphology were seen. The air-stable solid DD_2 Te₂ precursor precludes the necessity of phosphine reagents, which had been used in Cu_{2-x} Te syntheses reported previously.^{5,22}

To the authors' knowledge, this is the first example of a traditional nanocrystal synthesis for nanosheets of the layered vulcanite phase. Vulcanite has a modest presence in the literature, and a facile synthesis for this material enables further investigation of its potential photovoltaic characteristics or as a parent material for cation exchange. Since a nanocrystal synthesis for CuTe has not been reported previously with other more common tellurium-containing precursors, the solution phase reaction mechanism of the DD₂Te₂ appears to be unique. The distinctive dialkyl dichalcogenide reactivity highlighted here illustrates the ability of this family of precursors to access metastable and otherwise difficult-to-achieve phases.

Conflicts of interest

There are no conflicts to declare.

Acknowledgements

This work was financially supported by NSF grants EPS-1004083 and CHE-1905265 and the Vanderbilt Institute of Nanoscale Science and Engineering. EHR and KMD thank Susan Verberne-Sutton for guidance and thoughtful mentorship. The authors thank Ross Koby for assistance with DFT calculations. The authors thank Emil Hernańdez-Pagań and Sandra Rosenthal for helpful discussion regarding this project.

References

- 1 H. Li, M. Zanella, A. Genovese, M. Povia, A. Falqui, C. Giannini and L. Manna, *Nano Lett.*, 2011, 11, 4964–4970.
- 2 C. G. Sharp, A. D. P. Leach and J. E. Macdonald, *Nano Lett.*, 2020, DOI: 10.1021/acs.nanolett.0c03122. [ahead of print].

3 H. Li, R. Brescia, M. Povia, M. Prato, G. Bertoni, L. Manna and I. Moreels, *J. Am. Chem. Soc.*, 2013, 135, 12270–12278.

Nanoscale

- 4 R. Tu, Y. Xie, G. Bertoni, A. Lak, R. Gaspari, A. Rapallo, A. Cavalli, L. De Trizio and L. Manna, *J. Am. Chem. Soc.*, 2016, 138, 7082–7090.
- 5 W. Li, R. Zamani, P. Rivera Gil, B. Pelaz, M. Ibáñez, D. Cadavid, A. Shavel, R. A. Alvarez-Puebla, W. J. Parak, J. Arbiol and A. Cabot, *J. Am. Chem. Soc.*, 2013, 135, 7098–7101.
- 6 H. J. Yang, C. Y. Chen, F. W. Yuan and H. Y. Tuan, J. Phys. Chem. C, 2013, 117, 21955–21964.
- 7 I. Kriegel, C. Jiang, J. Rodríguez-Fernández, R. D. Schaller, D. V. Talapin, E. da Como and J. Feldmann, *J. Am. Chem. Soc.*, 2012, 134, 1583–1590.
- 8 T. Willhammar, K. Sentosun, S. Mourdikoudis, B. Goris, M. Kurttepeli, M. Bercx, D. Lamoen, B. Partoens, I. Pastoriza-Santos, J. Pérez-Juste, L. M. Liz-Marzán, S. Bals and G. Van Tendeloo, *Nat. Commun.*, 2017, 8, 1–7.
- 9 A. Comin and L. Manna, Chem. Soc. Rev., 2014, 43, 3957–3975.
- 10 A. C. Poulose, S. Veeranarayanan, M. S. Mohamed, R. R. Aburto, T. Mitcham, R. R. Bouchard, P. M. Ajayan, Y. Sakamoto, T. Maekawa and D. S. Kumar, *Sci. Rep.*, 2016, 6, 1–13.
- 11 X. Wang, Y. Ma, H. Chen, X. Wu, H. Qian, X. Yang and Z. Zha, *Colloids Surf.*, B, 2017, 152, 449–458.
- 12 C. Nethravathi, C. R. Rajamathi, M. Rajamathi, R. Maki, T. Mori, D. Golberg and Y. Bando, *J. Mater. Chem. A*, 2014, 2, 985–990.
- 13 C. Zhou, C. Dun, Q. Wang, K. Wang, Z. Shi, D. L. Carroll, G. Liu and G. Qiao, ACS Appl. Mater. Interfaces, 2015, 7, 21015–21020.
- 14 A. Ghosh, M. Mitra, D. Banerjee and A. Mondal, *RSC Adv.*, 2016, **6**, 22803–22811.
- 15 H. Wang, P. Zuo, A. Wang, S. Zhang, C. Mao, J. Song, H. Niu, B. Jin and Y. Tian, J. Alloys Compd., 2013, 581, 816– 820.
- 16 A. S. Pashinkin and V. A. Fedorov, *Inorg. Mater.*, 2003, **39**, 539–554.
- 17 J. L. F. Da Silva, S. H. Wei, J. Zhou and X. Wu, *Appl. Phys. Lett.*, 2007, **91**, 2–5.
- 18 O. Palchik, R. Kerner, Z. Zhu and A. Gedanken, *J. Solid State Chem.*, 2000, **154**, 530–534.
- 19 Y. Zhang, Z. P. Qiao and X. M. Chen, J. Mater. Chem., 2002, 12, 2747–2748.
- 20 L. Zhang, Z. Ai, F. Jia, L. Liu, X. Hu and J. C. Yu, *Chem. Eur. J.*, 2006, **12**, 4185–4190.
- 21 P. Kumar and K. Singh, Cryst. Growth Des., 2009, 9, 3089-3094.
- 22 E. Mugnaioli, M. Gemmi, R. Tu, J. David, G. Bertoni, R. Gaspari, L. De Trizio and L. Manna, *Inorg. Chem.*, 2018, 57, 10241–10248.
- 23 F. Pertlik, Mineral. Petrol., 2001, 71, 149-154.

- 24 K. Neyvasagam, N. Soundararajan, V. Venkatraman and V. Ganesan, *Vacuum*, 2007, **82**, 72–77.
- 25 Y. Yang, T. Wang, C. Liu, W. Li, J. Zhang, L. Wu, G. Zeng, W. Wang and M. Yu, *Vacuum*, 2017, 142, 181–185.
- 26 W. He, H. Zhang, Y. Zhang, M. Liu, X. Zhang and F. Yang, I. Nanomater., 2015, 2015, 1–5.
- 27 Z. Y. Aydın and S. Abacı, J. Solid State Electrochem., 2017, 21, 1417–1430.
- 28 R. L. Brutchey, Acc. Chem. Res., 2015, 48, 2918-2926.
- 29 B. A. Tappan, G. Barim, J. C. Kwok and R. L. Brutchey, *Chem. Mater.*, 2018, **30**, 5704–5713.
- 30 C.-C. Chen, A. B. Herhold, C. S. Johnson and A. P. Alivisatos, *Science*, 1997, **276**, 398–401.
- 31 E. A. Hernández-Pagán, E. H. Robinson, A. D. La Croix and J. E. Macdonald, *Chem. Mater.*, 2019, 31, 4619–4624.
- 32 G. Gariano, V. Lesnyak, R. Brescia, G. Bertoni, Z. Dang, R. Gaspari, L. De Trizio and L. Manna, *J. Am. Chem. Soc.*, 2017, 139, 9583–9590.
- 33 Y. Li, L. C. Silverton, R. Haasch and Y. Y. Tong, *Langmuir*, 2008, 24, 7048–7053.
- 34 Y. Guo, S. R. Alvarado, J. D. Barclay and J. Vela, *ACS Nano*, 2013, 7, 3616–3626.
- 35 J. M. Rhodes, C. A. Jones, L. B. Thal and J. E. Macdonald, *Chem. Mater.*, 2017, **29**, 8521–8530.
- 36 K. Stolze, A. Isaeva, F. Nitsche, U. Burkhardt, H. Lichte, D. Wolf and T. Doert, *Angew. Chem., Int. Ed.*, 2013, 52, 862– 865.
- 37 N. Stuhr-Hansen, K. Nørgaard, J. B. Christensen, L. K. Nielsen, T. Bjørnholm and M. Brust, *Nano Lett.*, 2001, 1, 189–191.
- 38 B. Mahler, N. Lequeux and B. Dubertret, *J. Am. Chem. Soc.*, 2010, 132, 953-959.
- 39 J. Huang, M. V. Kovalenko and D. V. Talapin, *J. Am. Chem. Soc.*, 2010, 132, 15866–15868.
- 40 Y. Gao and X. Peng, J. Am. Chem. Soc., 2014, 136, 6724-6732.
- 41 U. Soni, V. Arora and S. Sapra, *CrystEngComm*, 2013, **15**, 5458–5463.
- 42 A. L. Washington, M. E. Foley, S. Cheong, L. Quffa, C. J. Breshike, J. Watt, R. D. Tilley and G. F. Strouse, *J. Am. Chem. Soc.*, 2012, 134, 17046–17052.
- 43 S. Toso, S. Toso, Q. A. Akkerman, B. Martín-García, M. Prato, J. Zito, I. Infante, I. Infante, Z. Dang, A. Moliterni, C. Giannini, E. Bladt, I. Lobato, J. Ramade, S. Bals, S. Bals, J. Buha, D. Spirito, E. Mugnaioli, M. Gemmi, L. Manna and M. Gemmi, J. Am. Chem. Soc., 2020, 142, 10198–10211.
- 44 G. She, X. Zhang, W. Shi, Y. Cai, N. Wang, P. Liu and D. Chen, *Cryst. Growth Des.*, 2008, **8**, 1789–1791.
- 45 M. Pourbaix, *Atlas of Electrochemical Equilibria in Aqueous Solutions*, National Association of Corrosion Engineers, USA, 2nd Englis., 1974.